Supporting information

Mechanistic modelling of PSA dynamics shows potential for personalised prediction of radiation therapy outcome

Guillermo Lorenzo[a,b,*], Víctor M. Pérez-García[c,*], Alfonso Mariño[d], Luis A. Pérez Romasanta[e], Alessandro Reali[a], and Hector Gomez[f,g,h]

[a] *Dipartimento di Ingegneria Civile e Architettura, Università degli Studi di Pavia, via Ferrata 3, 27100 Pavia, Italy.*

[b] *Departamento de Matemáticas, Universidade da Coruña, Campus de Elviña s/n, 15071 A Coruña, Spain.*

[c] *Mathematical Oncology Laboratory (MôLAB), Universidad de Castilla-La Mancha, Edificio Politécnico, Avenida Camilo José Cela 3, 13071 Ciudad Real, Spain*

[d] *Servicio de Oncología Radioterápica, Centro Oncológico de Galicia, Calle Doctor Camilo Veiras 1, 15009 A Coruña, Spain*

[e] *Servicio de Oncología Radioterápica, Hospital Universitario de Salamanca, Paseo de San Vicente 58-182, 37007 Salamanca, Spain*

[f] *School of Mechanical Engineering, Purdue University, 585 Purdue Mall, West Lafayette, IN 47907, USA.*

[g] *Weldon School of Biomedical Engineering, Purdue University, 206 S. Martin Jischke Drive, West Lafayette, IN 47907, USA.*

[h] *Purdue Center for Cancer Research, Purdue University, 201 S. University Street, West Lafayette, IN 47907, USA.*

July 6, 2019

*Corresponding authors: guillermo.lorenzo@unipv.it, victor.perezgarcia@uclm.es

Notation	Definition
N	Number of tumour cells
N_0	Initial number of tumour cells, i.e., at time $t = t_0$
S	Number of surviving tumour cells
$\tilde{D}$	Number of irreversibly damaged tumour cells due to a certain radiation dose
D	Number of irreversibly damaged tumour cells accumulated since EBRT initiation
P	Serum PSA concentration
P_0	Initial serum PSA concentration, i.e., at time $t = t_0$
P_d	PSA at diagnosis
P_n	PSA nadir
$\widehat{P}$	Non-dimensional serum PSA concentration
$\widehat{v}_P$	Non-dimensional PSA velocity
ρ	Proportionality constant between P and N
t	Time
t_0	Time of first PSA value prior to EBRT
t_1	Time of EBRT initiation
t_{n_d}	Time of EBRT termination
$\widehat{t}$	Non-dimensional time
t_n	Time to PSA nadir
Δt_n	Time to PSA nadir since termination of EBRT
τ_n	Characteristic time of net proliferation of tumour cells before EBRT
τ_s	Characteristic time of net proliferation of surviving tumour cells
τ_d	Characteristic time of initiation of programmed-cell death of irreversibly damaged cells
τ_r	Periodicity of radiation doses in the periodic dose model
θ_1	Constant defined as $\theta_1 = e^{t_D\left(\frac{1}{\tau_n}-\frac{1}{\tau_s}\right)}$
θ_2	Constant defined as $\theta_2 = e^{t_D\left(\frac{1}{\tau_s}+\frac{1}{\tau_d}\right)}$
n_d	Number of radiation doses
R_d	Percentage of surviving tumour cells due to each radiation dose (generic and periodic dose model)
R_D	Percentage of surviving tumour cells due to the total radiation dose (single dose model)
α	Non-dimensional parameter
β	Non-dimensional parameter

Table S1. List of principal quantities of interest in the models presented in this study.

Annex S1: Comparative simulation study between the generic model and the periodic dose model

The aim of this annex is to describe an ancillary simulation to study to assess whether the periodic dose model (Section 2.2.2) can be used as a surrogate of the generic model (Section 2.2.1) in the context of the research presented in the main manuscript.

This study was designed as follows. We considered an artificial biochemically-relapsing patient characterised by $R_d = 0.93$, $\tau_d = 2$ mo, $\tau_s = 30$ mo undergoing all possible conventional (2 Gy/dose, n_d =38 doses) and hypofractionated (3 Gy/dose, n_d =21 doses) radiation plans delivering 2 to 5 doses/week, assuming that all doses are delivered the same days each week and the patient rests during the weekend. The constant time interval between radiation doses in the periodic dose model is given by $\tau_r = (t_{n_d} - t_1)/(n_d - 1)$. We focused on a biochemically-relapsing patient, because the corresponding dynamics are more complex and also feature the PSA decrease that would simply characterise a cured patient.

Each case of weekly EBRT plan consists of a seven-number binary code in which radiation is delivered the days marked with "1". We considered all possible combinations starting Monday to Friday and eliminating those plans that did not have two consecutive resting days (i.e., the weekend) as well as those which appeared twice for each fixed number of doses per week. All the possible weekly EBRT plans are summarised in Table S1 and the right-hand subpanels of Figure S1. Notice that in all cases there are at least two consecutive days in which the patient does not receive treatment, which would represent the weekend.

We computed the PSA dynamics corresponding to each weekly EBRT plan case using the generic model and the periodic dose model as described in the main manuscript. For the sake of simplicity and without losing generality, we assumed $t_1 = t_0 = 0$ and we studied the temporal evolution of PSA normalised with respect to its initial value at $t = 0$. This permitted us to focus on the decreasing and rising branches after EBRT obtained with each PSA dynamics model. To asses the difference between the dynamics provided by each model we used the mean absolute error (MAE) and the mean relative error (MRE), which defined as follows:

$$\mathrm{MAE} = \frac{1}{n_p}\sum_{i=1}^{n_p} |P_g(t_i) - P_p(t_i)|$$

$$\mathrm{MRE} = \frac{100}{n_p}\sum_{i=1}^{n_p} \left|\frac{P_g(t_i) - P_p(t_i)}{P_g(t_i)}\right|$$

where n_p is the number of time points used to compute MAE and MRE, t_i are the times of each of these sampling points, P_g is the serum PSA computed with the generic model, and P_p is the serum PSA computed with the periodic dose model. The sampling points were equally spaced between $t = 0$ and $t = 40$ mo with $\Delta t = 0.001$ mo.

Table S1 shows that the values of MAE and MRE are minimal for all EBRT weekly plans considered herein. Additionally, Figure S1 shows that the PSA dynamics predicted by the generic model and the periodic dose model are virtually indistinguishable for all cases involving 2, 3, 4, and 5 doses per week. Common radiation plans usually feature 4-5 doses per week, depending on the direct response of the patient to the treatment, programmed machine maintenance, or holidays. Our models did not only agree in all cases considering 4 or 5 doses per week, but also in the cases featuring 2 and 3 doses per week, in which the time period between doses used in the generic model may be more different than the corresponding τ_r in the periodic dose model. Therefore, we believe that this brief simulation study provides sufficient evidence to assume that the periodic dose model is practically equivalent to the generic model for the purposes of the research presented in the main manuscript.

Annex S2: Derivation of Eq. (9) from Eq. (7b)

In what follows, equation numbers make reference to the main text. The steps of the calculation are the following:

1. In Eq. (7b) substitute $t_i = t_1 + (i-1)\tau_r$ because in the periodic dose model the radiation doses are temporally equispaced (see first sentence of Section 2.2.2). Hence:

$$\begin{aligned} D_k(t) &= (1 - R_d)\left(\sum_{i=1}^{k} R_d^{i-1} e^{(t_i - t_1)\left(\frac{1}{\tau_s} + \frac{1}{\tau_d}\right)}\right) N_0 \theta_1 \theta_2 e^{-\frac{t}{\tau_d}} \\ &= (1 - R_d)\left(\sum_{i=1}^{k} R_d^{i-1} e^{(i-1)\tau_r\left(\frac{1}{\tau_s} + \frac{1}{\tau_d}\right)}\right) N_0 \theta_1 \theta_2 e^{-\frac{t}{\tau_d}} \end{aligned}$$

2. Now, the terms in the sum in the last equation define a geometric progression with general term $a_i = R_d^{i-1} e^{(i-1)\tau_r\left(\frac{1}{\tau_s} + \frac{1}{\tau_d}\right)}$. This general term can also be written as $a_i = r^{i-1}$, where r is the so-called common ratio $r = R_d e^{\tau_r\left(\frac{1}{\tau_s} + \frac{1}{\tau_d}\right)}$. Summing up the first k terms of the geometric progression for our case we get

$$\sum_{i=1}^{k} R_d^{i-1} e^{(i-1)\tau_r\left(\frac{1}{\tau_s} + \frac{1}{\tau_d}\right)} = \frac{1 - R_d^k e^{k\tau_r\left(\frac{1}{\tau_s} + \frac{1}{\tau_d}\right)}}{1 - R_d e^{\tau_r\left(\frac{1}{\tau_s} + \frac{1}{\tau_d}\right)}},$$

and then

$$D_k(t) = (1 - R_d)\frac{1 - R_d^k e^{k\tau_r\left(\frac{1}{\tau_s} + \frac{1}{\tau_d}\right)}}{1 - R_d e^{\tau_r\left(\frac{1}{\tau_s} + \frac{1}{\tau_d}\right)}} N_0 \theta_1 \theta_2 e^{-\frac{t}{\tau_d}},$$

which corresponds to the expression in Eq. (9) in the manuscript. If we substitute the definition of $S_k(t)$ from Eq. (7a) together with the definition of $D_k(t)$ for the periodic dose model in the general definition of $P_k(t)$ given in Eq. (5b), which we have derived herein and show in Eq. (9), we obtain Eq. (10).

Case	Weekly EBRT plan	Conventional EBRT				Hypofractionated EBRT			
		Duration (d)	τ_r (d)	MAE (1)	MRE (%)	Duration (d)	τ_r (d)	MAE (1)	MRE (%)
2 doses/week									
1	1100000	128	3.46	$6.58{\cdot}10^{-4}$	0.149	71	3.55	$1.11{\cdot}10^{-4}$	0.204
2	1010000	129	3.49	$4.99{\cdot}10^{-4}$	0.125	71	3.55	$7.77{\cdot}10^{-4}$	0.143
3	1001000	130	3.51	$3.39{\cdot}10^{-4}$	0.100	71	3.55	$4.40{\cdot}10^{-4}$	0.083
4	1000100	131	3.54	$2.12{\cdot}10^{-4}$	0.078	71	3.55	$1.24{\cdot}10^{-4}$	0.025
5	1000010	132	3.57	$2.59{\cdot}10^{-4}$	0.077	71	3.55	$2.37{\cdot}10^{-4}$	0.038
6	1000001	133	3.59	$3.65{\cdot}10^{-4}$	0.086	71	3.55	$5.75{\cdot}10^{-4}$	0.098
3 doses/week									
1	1110000	86	2.32	$9.97{\cdot}10^{-4}$	0.267	45	2.25	$4.56{\cdot}10^{-4}$	0.078
2	1101000	86	2.32	$7.35{\cdot}10^{-4}$	0.195	46	2.30	$5.03{\cdot}10^{-4}$	0.089
3	1100100	86	2.32	$4.72{\cdot}10^{-4}$	0.124	47	2.35	$5.50{\cdot}10^{-4}$	0.100
4	1100010	86	2.32	$2.10{\cdot}10^{-4}$	0.052	48	2.40	$5.97{\cdot}10^{-4}$	0.111
5	1100001	86	2.32	$0.77{\cdot}10^{-4}$	0.023	49	2.45	$6.43{\cdot}10^{-4}$	0.122
6	1011000	87	2.35	$7.02{\cdot}10^{-4}$	0.199	46	2.30	$2.67{\cdot}10^{-4}$	0.047
7	1010100	87	2.35	$4.39{\cdot}10^{-4}$	0.128	47	2.35	$3.14{\cdot}10^{-4}$	0.058
8	1010010	87	2.35	$1.77{\cdot}10^{-4}$	0.056	48	2.40	$3.61{\cdot}10^{-4}$	0.069
9	1010001	87	2.35	$0.88{\cdot}10^{-4}$	0.016	49	2.45	$4.11{\cdot}10^{-4}$	0.080
10	1001100	88	2.38	$4.08{\cdot}10^{-4}$	0.132	47	2.35	$0.82{\cdot}10^{-4}$	0.016
11	1001010	88	2.38	$1.90{\cdot}10^{-4}$	0.065	48	2.40	$1.49{\cdot}10^{-4}$	0.029
12	1001001	88	2.38	$1.36{\cdot}10^{-4}$	0.020	49	2.45	$2.22{\cdot}10^{-4}$	0.043
13	1000110	89	2.41	$2.51{\cdot}10^{-4}$	0.079	48	2.40	$1.11{\cdot}10^{-4}$	0.016
14	1000101	89	2.41	$2.16{\cdot}10^{-4}$	0.037	49	2.45	$1.08{\cdot}10^{-4}$	0.014
15	1000011	90	2.43	$2.95{\cdot}10^{-4}$	0.053	49	2.45	$3.01{\cdot}10^{-4}$	0.047
4 doses/week									
1	1111000	65	1.76	$9.55{\cdot}10^{-4}$	0.264	36	1.80	$9.95{\cdot}10^{-4}$	0.183
2	1110100	65	1.76	$7.67{\cdot}10^{-4}$	0.212	36	1.80	$8.40{\cdot}10^{-4}$	0.155
3	1110010	65	1.76	$5.79{\cdot}10^{-4}$	0.160	36	1.80	$6.86{\cdot}10^{-4}$	0.126
4	1110001	65	1.76	$3.90{\cdot}10^{-4}$	0.107	36	1.80	$5.31{\cdot}10^{-4}$	0.098
5	1101100	65	1.76	$5.65{\cdot}10^{-4}$	0.157	36	1.80	$6.75{\cdot}10^{-4}$	0.125
6	1101001	65	1.76	$1.88{\cdot}10^{-4}$	0.052	36	1.80	$3.65{\cdot}10^{-4}$	0.068
7	1100110	65	1.76	$1.75{\cdot}10^{-4}$	0.050	36	1.80	$3.54{\cdot}10^{-4}$	0.066
8	1100101	65	1.76	$0.19{\cdot}10^{-4}$	0.003	36	1.80	$1.99{\cdot}10^{-4}$	0.038
9	1100011	65	1.76	$2.20{\cdot}10^{-4}$	0.058	36	1.80	$0.55{\cdot}10^{-4}$	0.010
10	1011100	66	1.78	$5.94{\cdot}10^{-4}$	0.175	36	1.80	$4.97{\cdot}10^{-4}$	0.093
11	1011001	66	1.78	$2.19{\cdot}10^{-4}$	0.070	36	1.80	$1.88{\cdot}10^{-4}$	0.036
12	1010011	66	1.78	$1.88{\cdot}10^{-4}$	0.040	36	1.80	$1.45{\cdot}10^{-4}$	0.024
13	1001110	67	1.81	$2.74{\cdot}10^{-4}$	0.090	36	1.80	$0.55{\cdot}10^{-4}$	0.008
14	1001101	67	1.81	$1.69{\cdot}10^{-4}$	0.047	36	1.80	$1.57{\cdot}10^{-4}$	0.026
15	1001011	67	1.81	$1.59{\cdot}10^{-4}$	0.022	36	1.80	$3.24{\cdot}10^{-4}$	0.056
16	1000111	68	1.84	$2.07{\cdot}10^{-4}$	0.035	36	1.80	$5.02{\cdot}10^{-4}$	0.088
5 doses/week									
1	1111100	52	1.37	$6.73{\cdot}10^{-4}$	0.187	29	1.45	$7.75{\cdot}10^{-4}$	0.143
2	1111001	52	1.37	$3.86{\cdot}10^{-4}$	0.106	29	1.45	$5.37{\cdot}10^{-4}$	0.099
3	1110011	52	1.37	$0.78{\cdot}10^{-4}$	0.022	29	1.45	$2.82{\cdot}10^{-4}$	0.053
4	1100111	54	1.42	$2.55{\cdot}10^{-4}$	0.082	29	1.45	$0.39{\cdot}10^{-4}$	0.006
5	1001111	54	1.42	$1.31{\cdot}10^{-4}$	0.019	29	1.45	$2.86{\cdot}10^{-4}$	0.049

Table S2. Quantitative comparison between the simulated PSA evolution with the general model and the periodic dose model, showing that they provide virtually equivalent PSA curves. These simulations correspond to the PSA dynamics of an artificial biochemically-relapsing patient ($R_d = 0.93$, $\tau_d = 2$ mo, $\tau_s = 30$ mo) undergoing all possible conventional (2 Gy/dose, n_d =38 doses) and hypofractionated (3 Gy/dose, n_d =21 doses) radiation plans delivering 2 to 5 doses/week, assuming that all doses are delivered the same days each week and the patient rests during the weekend. The weekly EBRT plan consists of a seven-number binary code in which radiation is delivered the days marked with "1". The constant time interval between radiation doses in the periodic dose model is given by $\tau_r = (t_{n_d} - t_1)/(n_d - 1)$. This table shows the mean absolute error (MAE) between the periodic dose model and the general model, as well as the mean relative error (MRE) with respect to the PSA curve provided by the general model for each simulation case.

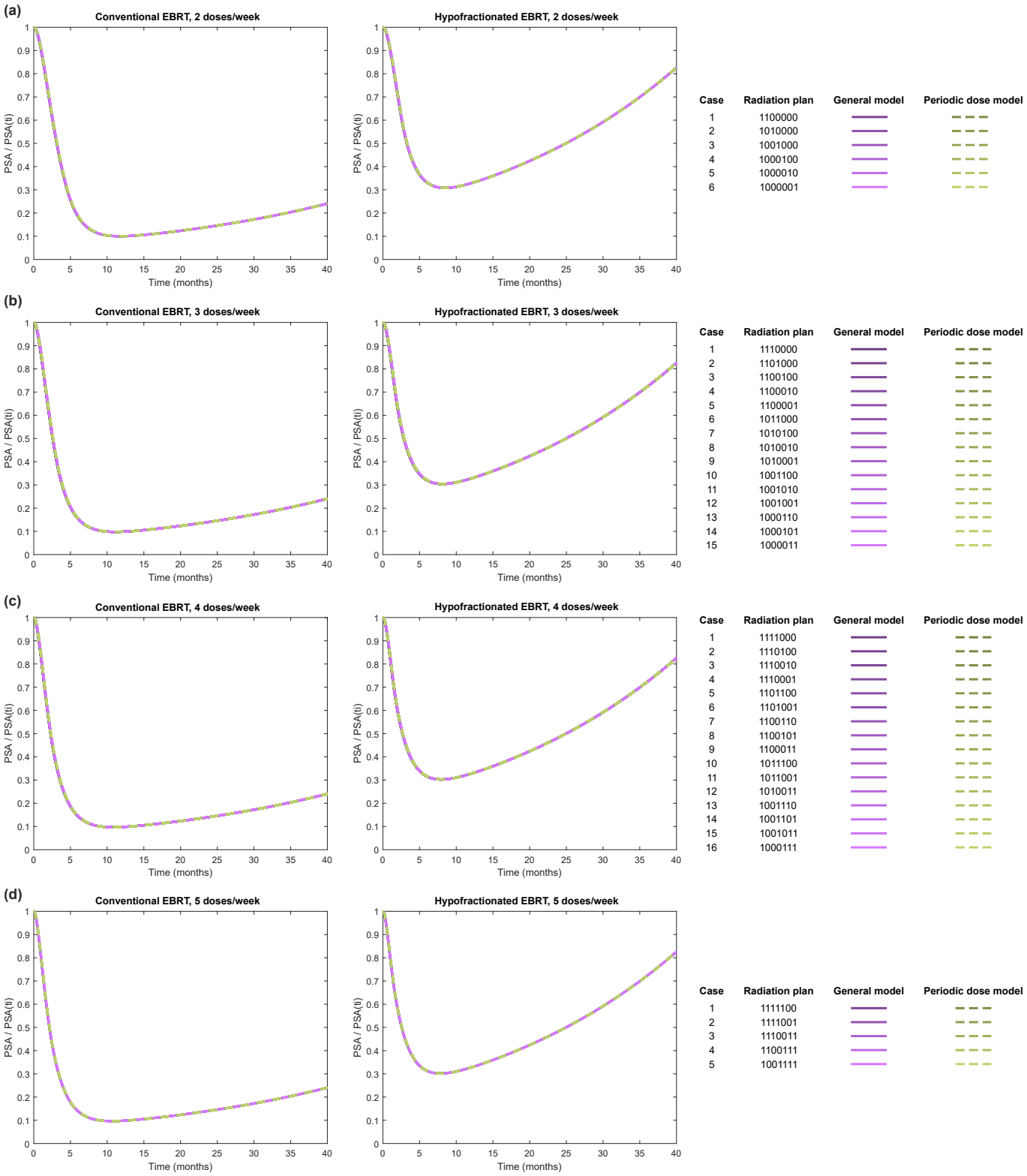

Figure S1. The periodic dose model is virtually equivalent to the general model. This figure shows a comparative of the solutions obtained with each model for an artificial biochemically-relapsing patient ($R_d = 0.93$, $\tau_d = 2$ mo, $\tau_s = 30$ mo) undergoing all possible conventional (2 Gy/dose, 38 doses) and hypofractionated (3 Gy/dose, 21 doses) radiation plans delivering 2 (a), 3 (b), 4 (c), and 5 doses/week (d), assuming that all doses are delivered the same days each week and the patient rests during the weekend. The plotted PSA curves for each model correspond to the simulation cases in Table S1. For each subfigure, the first plot corresponds to the conventional plans and the second plot to the hypofractionated plans. Time scale is shifted such that $t = 0$ corresponds to the onset of EBRT, and PSA is normalised with respect to PSA(0). Notice that all simulated PSA dynamics represented in each plot are indistinguishable, regardless of the radiation plan and mathematical model. As we deliver more doses per week, the PSA decay following EBRT is steeper and the time to PSA nadir is shorter.

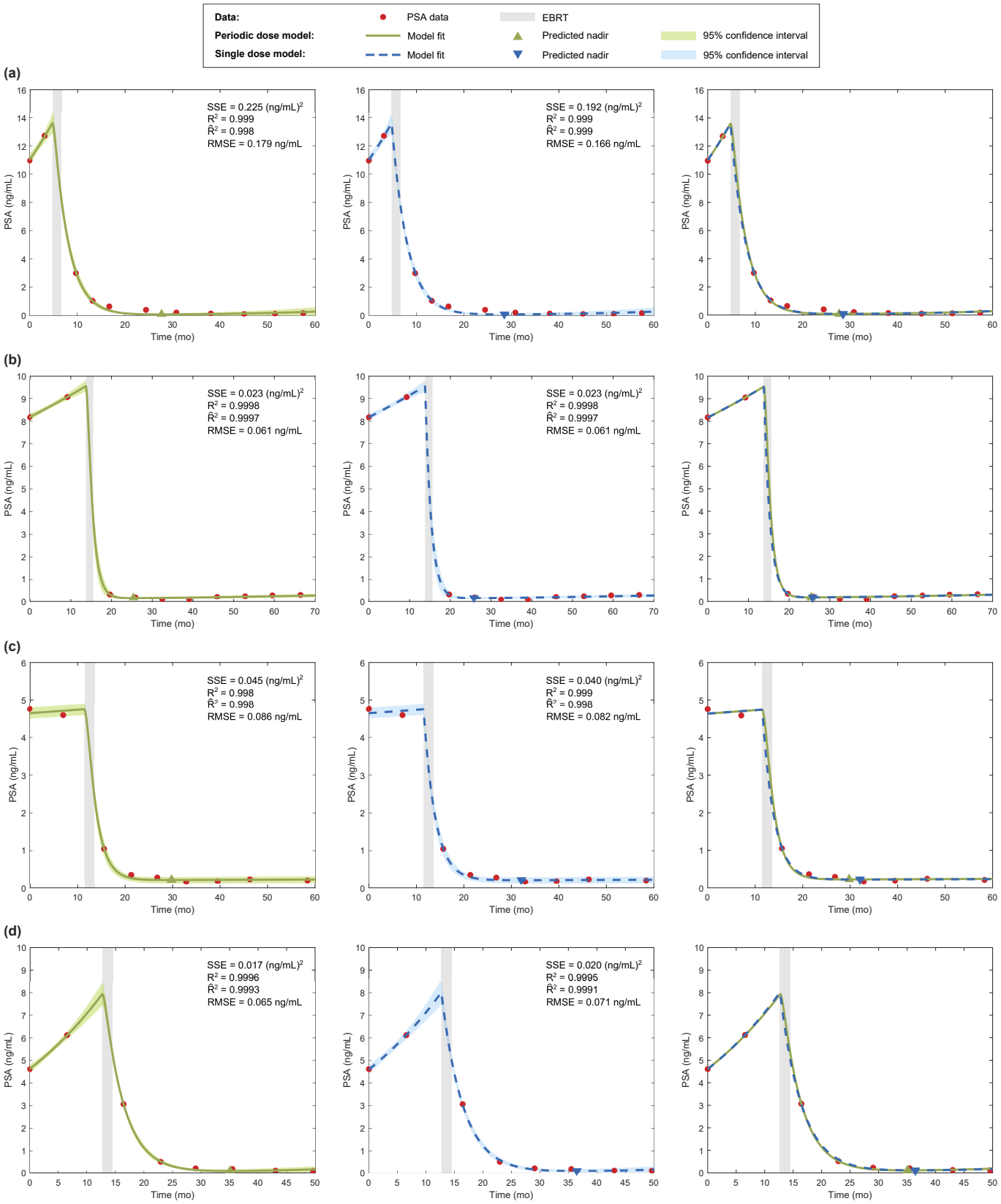

Figure S2. Examples of superior fitting results. These four patients (a-d) show several PSA values with minimal fluctuations distributed at approximately even intervals around the time of EBRT, when major changes to PSA dynamics take place. In particular, notice that these cases feature at least two PSA data before EBRT and two PSA data in the first year after concluding EBRT. For each patient (a-d), each row shows respectively the fit provided by the periodic dose model, the fit obtained with the single dose model, and a comparison of the fits computed with either model. The shaded areas along the model fits in the first two subfigures of each row depict the corresponding 95% confidence interval of the model fit. PSA values are depicted as red bullets and the duration of EBRT is shaded in light gray.

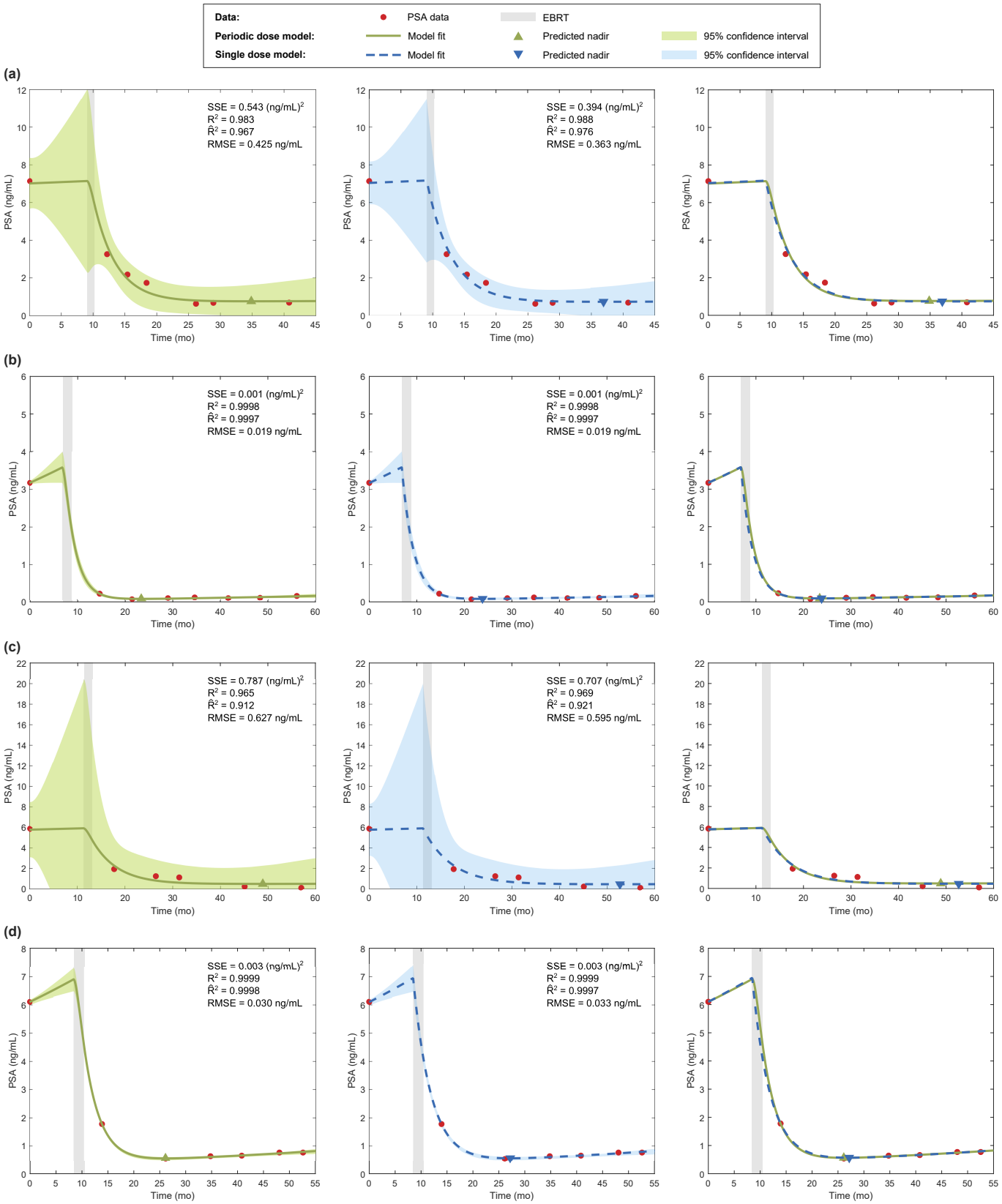

Figure S3. Lack of data close to EBRT may compromise model fitting. (a) A shortage of PSA data prior to radiotherapy may worsen the goodness of fit and increase the uncertainty of the model interpolation. (b) Lack of pre-EBRT data does not necessarily affect the accuracy of model fitting. The time intervals between the available points and with respect EBRT may still permit a good interpolation, provided that PSA data does not exhibit large fluctuations. (c) The scarcity of PSA data in the first years following termination of EBRT may also deteriorate the accuracy of model fit. (d) A good distribution of minimally fluctuating PSA values in time before and after EBRT may enable an optimal interpolation of the models, even when the number of data points is minimal around the time of EBRT. For each patient (a-d), each row shows respectively the fit provided by the periodic dose model, the fit obtained with the single dose model, and a comparison of the fits computed with either model. The shaded areas along the model fits in the first two subfigures of each row depict the corresponding 95% confidence interval of the model fit. PSA values are depicted as red bullets and the duration of EBRT is shaded in light gray.

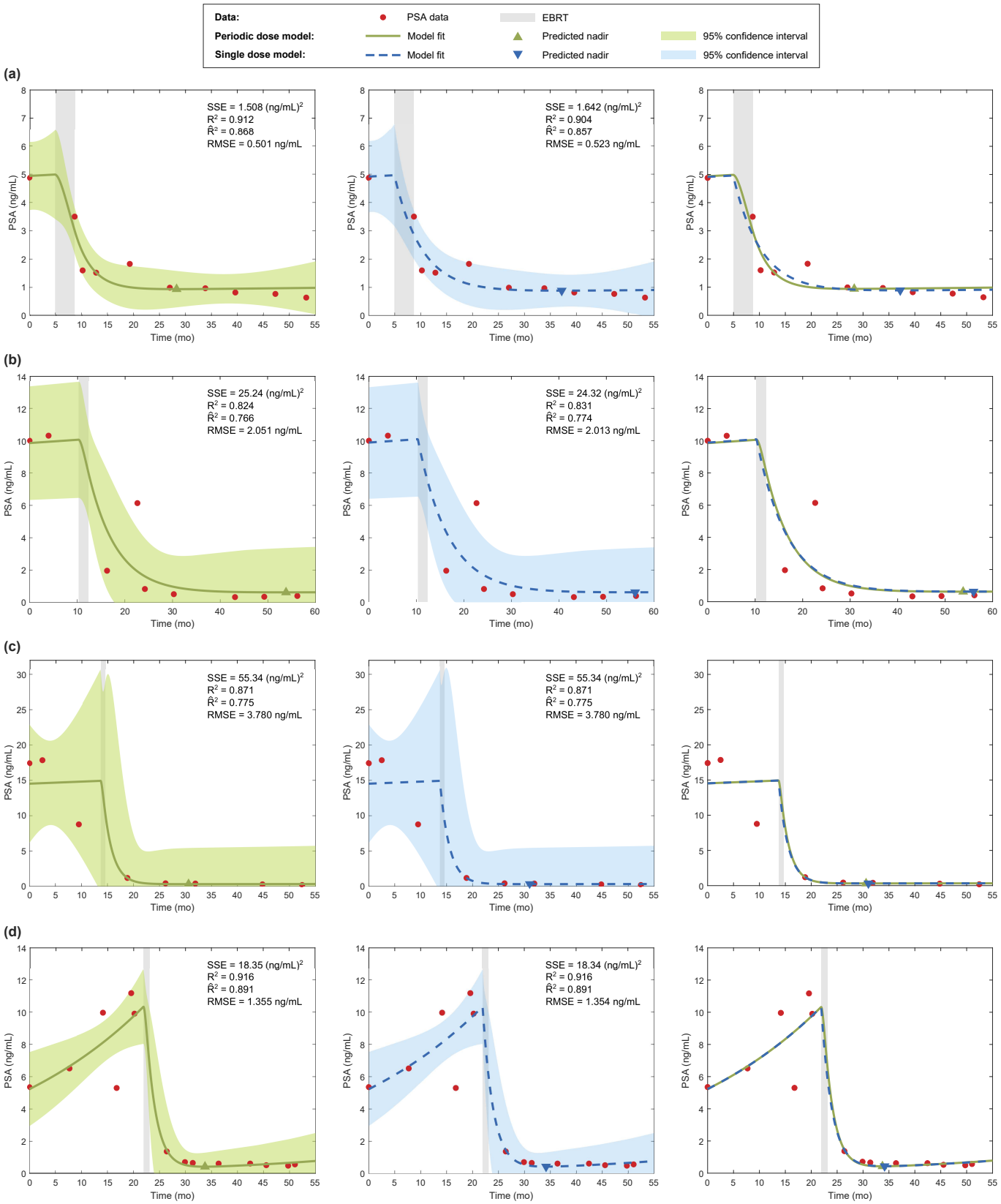

Figure S4. PSA fluctuations have a great impact on fitting results. Notice that patients (a) and (b) show a PSA bounce in the first year after conclusion of EBRT. (a) Oscillations in PSA data reduce the accuracy of model fitting. (b) Large PSA fluctuations produce a major impact on goodness of model fitting. (c) Scarcity of PSA data showing high oscillations leads to poorer model fitting. (d) The availability of multiple PSA data may counteract the uncertainty introduced by PSA fluctuations. For each patient (a-d), each row shows respectively the fit provided by the periodic dose model, the fit obtained with the single dose model, and a comparison of the fits computed with either model. The shaded areas along the model fits in the first two subfigures of each row depict the corresponding 95% confidence interval of the model fit. PSA values are depicted as red bullets and the duration of EBRT is shaded in light gray.

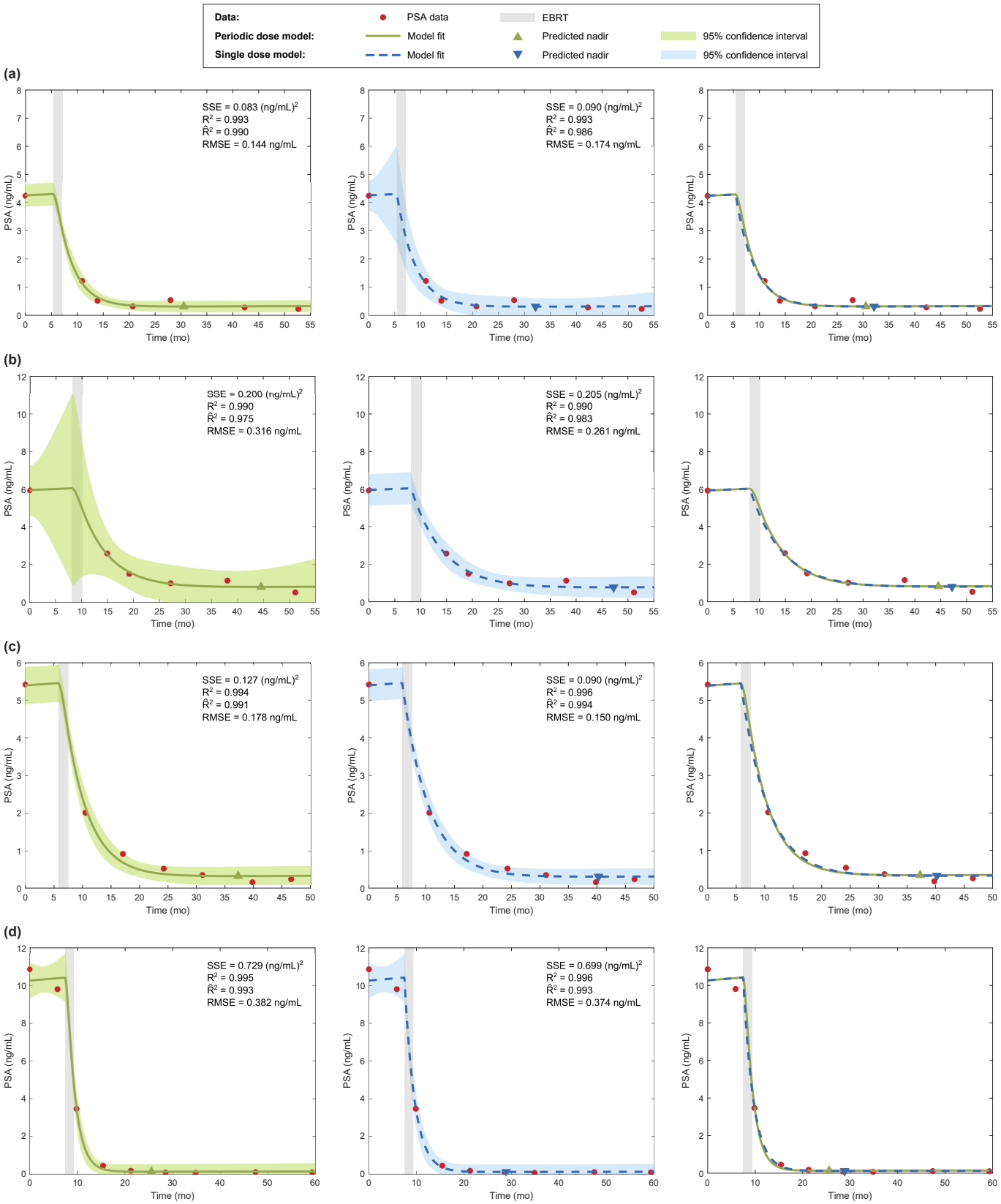

Figure S5. An estimated $\tau_s \approx 500$ does not compromise the accuracy of model fitting. (a-b) Absence of enough data to precisely estimate τ_s may locally increase the uncertainty of the model fit and slightly reduce the goodness-of-fit statistics. (c) In some cases, $\tau_s \approx 500$ had a negligible impact on the fitting results. (d) Patients with only two decreasing PSA values prior to EBRT also showed $\tau_s \approx 500$, but this issue did not necessarily jeopardise model interpolation. For each patient (a-d), each row shows respectively the fit provided by the periodic dose model, the fit obtained with the single dose model, and a comparison of the fits computed with either model. The shaded areas along the model fits in the first two subfigures of each row depict the corresponding 95% confidence interval of the model fit. PSA values are depicted as red bullets and the duration of EBRT is shaded in light gray.